

Canonical sampling through velocity rescaling

Cite as: J. Chem. Phys. **126**, 014101 (2007); <https://doi.org/10.1063/1.2408420>

Submitted: 22 September 2006 . Accepted: 17 November 2006 . Published Online: 03 January 2007

Giovanni Bussi, Davide Donadio, and Michele Parrinello



View Online



Export Citation

ARTICLES YOU MAY BE INTERESTED IN

[Molecular dynamics simulations at constant pressure and/or temperature](#)

The Journal of Chemical Physics **72**, 2384 (1980); <https://doi.org/10.1063/1.439486>

[A unified formulation of the constant temperature molecular dynamics methods](#)

The Journal of Chemical Physics **81**, 511 (1984); <https://doi.org/10.1063/1.447334>

[A consistent and accurate ab initio parametrization of density functional dispersion correction \(DFT-D\) for the 94 elements H-Pu](#)

The Journal of Chemical Physics **132**, 154104 (2010); <https://doi.org/10.1063/1.3382344>

The Journal
of Chemical Physics

2018 EDITORS' CHOICE

READ NOW!

Canonical sampling through velocity rescaling

Giovanni Bussi,^{a)} Davide Donadio, and Michele Parrinello

Computational Science, Department of Chemistry and Applied Biosciences, ETH Zürich, USI Campus, Via Giuseppe Buffi 13, CH-6900 Lugano, Switzerland

(Received 22 September 2006; accepted 17 November 2006; published online 3 January 2007)

The authors present a new molecular dynamics algorithm for sampling the canonical distribution. In this approach the velocities of all the particles are rescaled by a properly chosen random factor. The algorithm is formally justified and it is shown that, in spite of its stochastic nature, a quantity can still be defined that remains constant during the evolution. In numerical applications this quantity can be used to measure the accuracy of the sampling. The authors illustrate the properties of this new method on Lennard-Jones and TIP4P water models in the solid and liquid phases. Its performance is excellent and largely independent of the thermostat parameter also with regard to the dynamic properties. © 2007 American Institute of Physics. [DOI: [10.1063/1.2408420](https://doi.org/10.1063/1.2408420)]

I. INTRODUCTION

Controlling the temperature and assessing the quality of the trajectories generated are crucial issues in any molecular dynamics simulation.^{1,2} Let us first recall that in conventional molecular dynamics the microcanonical ensemble *NVE* is generated due to the conservation laws of Hamilton's equations. In this ensemble the number of particles *N*, the volume *V*, and the energy *E* are kept constant. In the early days of molecular dynamics the temperature was controlled by rescaling the velocities until the system was equilibrated at the target temperature. Energy conservation was also closely monitored in order to check that the correct *NVE* ensemble was being sampled and as a way of choosing the integration time step. Furthermore, energy conservation provided a convenient tool for controlling that the code was free from obvious bugs.

Only in 1980, in a landmark paper,³ Andersen suggested that ensembles other than the microcanonical one could be generated in a molecular dynamics run in order to better mimic the experimental conditions. Here we only discuss his proposal for generating the canonical ensemble *NVT*, in which the temperature *T* rather than the energy *E* is fixed. Andersen's prescription was rather simple: during the simulation a particle is chosen randomly and its velocity extracted from the appropriate Maxwell distribution. While formally correct, Andersen's thermostat did not become popular. A supposedly poor efficiency was to blame, as well as the fact that discontinuities in the trajectories were introduced. However, its major drawback was probably the fact that one had to deal with an algorithm without the comforting notion of a conserved quantity on which to rely. Another type of stochastic dynamics which leads to a canonical distribution is Langevin dynamics.⁴ Such a dynamics is not often used because it does not have an associated conserved quantity, the integration time step is difficult to control, and the trajectories lose their physical meaning unless the friction coefficient is small. For similar reasons, an algorithm⁵ which is close to

the simplified version of ours discussed in Sec. II A has been even less popular. Inspired by the extended Lagrangian approach introduced in Andersen's paper to control the external pressure, Nosé introduced his by now famous thermostat.⁶ Differently from Andersen's thermostat, the latter allowed to control the temperature without using random numbers. Furthermore, associated with Nosé's dynamics there was a conserved quantity. Thus it is not surprising that Nosé's thermostat is widely used, especially in the equivalent form suggested by Hoover.⁷ However, Nosé thermostat can exhibit nonergodic behavior. In order to compensate for this shortcoming, the introduction of chains of thermostats was suggested,⁸ but this spoils the beauty and simplicity of the theory and needs extra tuning.

Alternative thermostats were suggested such as that of Evans and Morriss⁹ in which the total kinetic energy is kept strictly constant. This leads to a well defined ensemble, the so-called isokinetic ensemble, which, however, cannot be experimentally realized. Another very popular thermostat is that of Berendsen *et al.*¹⁰ In this approach Hamilton's equations are supplemented by a first-order equation for the kinetic energy, whose driving force is the difference between the instantaneous kinetic energy and its target value. Berendsen's thermostat is stable, simple to implement, and physically appealing; however, it has no conserved quantity and is not associated with a well defined ensemble, except in limiting cases. In spite of this, it is rather widely used.

In this paper we propose a new method for controlling the temperature that removes many of the difficulties mentioned above. Our method is an extension of the Berendsen thermostat to which a properly constructed random force is added, so as to enforce the correct distribution for the kinetic energy. A relaxation time of the thermostat can be chosen such that the dynamic trajectories are not significantly affected. We show that it leads to the correct canonical distribution and that there exists a unified scheme in which Berendsen's, Nosé's, and our thermostat can be formulated. A remarkable result is that a quantity can be defined which is constant and plays a role similar to that of the energy in the microcanonical ensemble. Namely, it can be used to verify

^{a)}Electronic mail: gbugsi@ethz.ch

how much our numerical procedure generates configurations that belong to the desired NVT ensemble and to provide a guideline for the choice of the integration time step. It must be mentioned that all the algorithms presented here are extremely easy to implement.

In Sec. II we shall first present a simpler version of our algorithm which is an extension of the time honored velocity rescaling. Later we shall describe its more general formulation, followed by a theoretical analysis of the new approach, a comparison with other schemes, and a discussion of the errors derived from the integration with a finite time step. The following Secs. III and IV are devoted to numerical checks of the theory and to a final discussion, respectively.

II. THEORY

A. A canonical velocity-rescaling thermostat

In its simplest formulation, the velocity-rescaling method consists in multiplying the velocities of all the particles by the same factor α , calculated by enforcing the total kinetic energy K to be equal to the average kinetic energy at the target temperature, $\bar{K} = N_f/2\beta$, where N_f is the number of degrees of freedom and β is the inverse temperature. Thus, the rescaling factor α for the velocities is obtained as

$$\alpha = \sqrt{\frac{\bar{K}}{K}}. \quad (1)$$

Since the same factor is used for all the particles, there is neither an effect on constrained bond lengths nor on the center of mass motion. This operation is usually performed at a predetermined frequency during equilibration, or when the kinetic energy exceeds the limits of an interval centered around the target value. The sampled ensemble is not explicitly known but, since in the thermodynamic limit the average properties do not depend on the ensemble chosen, even this very simple algorithm can be used to produce useful results. However, for small systems or when the observables of interest are dependent on the fluctuations rather than on the averages, this method cannot be used. Moreover, it is questionable to assume that this algorithm can be safely combined with other methods which require canonical sampling, such as replica-exchange molecular dynamics.¹¹

We propose to modify the way the rescaling factor is calculated, so as to enforce a canonical distribution for the kinetic energy. Instead of forcing the kinetic energy to be exactly equal to \bar{K} , we select its target value K_t with a stochastic procedure aimed at obtaining the desired ensemble. To this effect we evaluate the velocity-rescaling factor as

$$\alpha = \sqrt{\frac{K_t}{K}}, \quad (2)$$

where K_t is drawn from the canonical equilibrium distribution for the kinetic energy:

$$\bar{P}(K_t) dK_t \propto K_t^{(N_f/2-1)} e^{-\beta K_t} dK_t. \quad (3)$$

This is equivalent to the method proposed by Heyes,⁵ where one enforces the distribution in Eq. (3) by a Monte Carlo procedure. Between rescalings we evolve the system using

Hamilton's equations. The number of integration time steps can be fixed or randomly varied. Both the Hamiltonian evolution and the velocity rescaling leave a canonical probability distribution unaltered. Under the condition that the Hamiltonian evolution is ergodic in the microcanonical ensemble, it follows that our method samples the canonical ensemble.¹² More precisely, Hamilton's equations sample a phase-space surface with fixed center of mass and, for non-periodic systems, zero angular momentum. Since the rescaling procedure does not change these quantities, our algorithm samples only the corresponding slice of the canonical ensemble. We shall neglect this latter effect here and in the following as we have implicitly done in Eq. (3).

B. A more elaborate approach

The procedure described above is very simple but disturbs considerably the velocities of the particles. In fact, each time the rescaling is applied, the moduli of the velocities will exhibit a fast fluctuation with relative magnitude $\sqrt{1/N_f}$. Thus, we propose a smoother approach in which the rescaling procedure is distributed among a number of time steps. This new scheme is somehow related to what previously described in the same way as the Berendsen thermostat is related to standard velocity rescaling.

First we note that it is not necessary to draw K_t from the distribution in Eq. (3) at each time step: the only requirement is that the random changes in the kinetic energy leave a canonical distribution unchanged. In particular, the choice of K_t can be based on the previous value of K so as to obtain a smoother evolution. We propose a general way of doing this by applying the following prescriptions:

- (1) Evolve the system for a single time step with Hamilton's equations, using a time-reversible area-preserving integrator such as velocity Verlet.¹³
- (2) Calculate the kinetic energy.
- (3) Evolve the kinetic energy for a time corresponding to a single time step using an auxiliary continuous stochastic dynamics.
- (4) Rescale the velocities so as to enforce this new value of the kinetic energy.

The choice of the stochastic dynamics has some degree of arbitrariness, the only constraint being that it has to leave the canonical distribution in Eq. (3) invariant. Here we choose this dynamics by imposing that it is described by a first-order differential equation in K . Since the auxiliary dynamics on K is one dimensional, its associated Fokker-Planck equation¹⁴ must exhibit a zero-current solution. It can be shown that under these conditions the most general form is

$$dK = \left(D(K) \frac{\partial \log \bar{P}}{\partial K} + \frac{\partial D(K)}{\partial K} \right) dt + \sqrt{2D(K)} dW, \quad (4)$$

where $D(K)$ is an arbitrary positive definite function of K , dW a Wiener noise, and we are using the Itoh convention.¹⁴ Inserting the distribution of Eq. (3) in this equation, one finds

$$dK = \left(\frac{N_f D(K)}{2\bar{K}K} (\bar{K} - K) - \frac{D(K)}{K} + \frac{\partial D(K)}{\partial K} \right) dt + \sqrt{2D(K)} dW, \quad (5)$$

which can be used to generate the correct canonical distribution. This result is independent of the choice of the function $D(K)$, but different choices can lead to different speeds of equilibration. Here we choose

$$D(K) = \frac{2K\bar{K}}{N_f\tau}, \quad (6)$$

where the arbitrary parameter τ has the dimension of time and determines the time scale of the thermostat such as in Berendsen's formulation. This leads to a very transparent expression for the auxiliary dynamics

$$dK = (\bar{K} - K) \frac{dt}{\tau} + 2 \sqrt{\frac{K\bar{K}}{N_f}} \frac{dW}{\sqrt{\tau}}. \quad (7)$$

Without the stochastic term this equation reduces to that of the standard thermostat of Berendsen. In the limit $\tau=0$, the stochastic evolution is instantly thermalized and this algorithm reduces exactly to the stochastic velocity-rescaling approach described in Sec. II A. On the other hand, for $\tau \rightarrow \infty$, the Hamiltonian dynamics is recovered. When a system is far from equilibrium, the deterministic part in Eq. (7) dominates and our algorithm leads to fast equilibration like the Berendsen's thermostat. Once the equilibrium is reached, the proper canonical ensemble is sampled, at variance with Berendsen's thermostat.

There is no need to apply additional self-consistency procedures to enforce rigid bond constraints, as in the case of Andersen's thermostat, since the choice of a single rescaling factor for all the atoms automatically preserves bond lengths. Furthermore, the total linear momentum and, for nonperiodic systems, the angular momentum are conserved. The formalism can also be trivially extended to thermalize independently different parts of the system, e.g., solute and solvent, even using different parameters τ for the different subsystems. Interestingly, dissipative particle dynamics¹⁵ can be included in our scheme if different thermostats are applied to all the particle pairs that are within a given distance.

We have already noted that Berendsen's thermostat can be recovered from ours by switching off the noise. Also Nosé's thermostat can be recast in a form that parallels our formulation. To this effect, it is convenient to rewrite the auxiliary variable ξ of the Nosé-Hoover thermostat in adimensional form $\xi = \zeta/\tau$ and the mass of the thermostat as $(N_f/\beta)\tau^2$. In our scheme, Nosé-Hoover dynamics is obtained through these auxiliary equations for ζ and K :

$$dK = -2\zeta K \frac{dt}{\tau}, \quad (8a)$$

$$d\zeta = \left(\frac{K}{\bar{K}} - 1 \right) \frac{dt}{\tau}. \quad (8b)$$

The corresponding Liouville equation for the probability distribution $P(K, \zeta)$ is

$$\tau \frac{\partial P(K, \zeta; t)}{\partial t} = 2\zeta P + 2\zeta K \frac{\partial P(K, \zeta; t)}{\partial K} - \left(\frac{K}{\bar{K}} - 1 \right) \frac{\partial P(K, \zeta; t)}{\partial \zeta}, \quad (9)$$

which is stationary for

$$\bar{P}(K, \zeta) dK d\zeta \propto K^{(N_f/2-1)} e^{-\beta K} e^{-N_f \zeta^2/2} dK d\zeta \quad (10)$$

which is the desired distribution. By comparing this formulation of the Nosé-Hoover thermostat with our scheme, we see that the variable ζ plays the same role as the noise. In the Nosé-Hoover scheme, the chaotic nature of the coupled equations of motion leads to a stochastic ζ . When the system to be thermostated is poorly ergodic, ζ is no longer stochastic and a chain of thermostats is needed.⁸

C. Controlling the integration time step

When integrating the equations of motion using a finite time step, a technical but important issue is the choice of an optimal value for the time step. The usual paradigm is to check if the constants of motion are properly conserved. For example, in the microcanonical ensemble, sampled using the Hamilton's equations, the check is done on the total energy of the system which is given by the Hamiltonian $H(x)$, where $x=(p, q)$ is a point in phase space. When the Nosé-Hoover thermostat is used, the expression for the conserved quantity $H_{\text{Nosé}}$ is more complex and can be recast in the form

$$H_{\text{Nosé}} = H(x) + \frac{N_f}{\beta} \left(\frac{\zeta^2}{2} + \int_0^t \frac{dt'}{\tau} \zeta(t') \right). \quad (11)$$

In this section we propose a quantity that can play the same role for our thermostat, even though we are dealing with a stochastic process.

Let us consider a deterministic or stochastic dynamics aimed at sampling a given probability distribution $\bar{P}(x)$. It is convenient to consider a discrete form of dynamics. This is not a major restriction and, after all, on the computer any dynamics is implemented as a discrete process. Starting from a point x_0 in the phase space, we want to generate a sequence of points x_1, x_2, \dots , distributed according to a probability as close as possible to $\bar{P}(x)$. Let $M(x_{i+1} \leftarrow x_i) dx_{i+1}$ be the conditional probability of reaching the point x_{i+1} given that the system is at x_i . In order to calculate statistical averages which are correct independent of M , each visited point has to be weighted by w_i which measures the probability that x_i is in the target ensemble. The ratio between the weights of successive points is

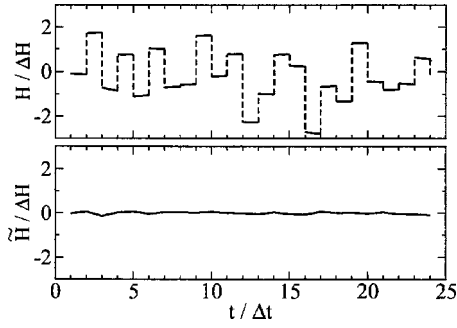


FIG. 1. Schematic time series for H (upper) and \tilde{H} (lower), in units of the root-mean-square fluctuation of H . Time is in unit of the integration time step. The solid lines represent the increments due to the velocity Verlet step, which is almost energy preserving. The dashed lines represent the increments due to the velocity rescaling. Since only the changes due to the velocity Verlet steps are accumulated into \tilde{H} , this quantity is almost constant. On the other hand, H has the proper distribution.

$$\frac{w_{i+1}}{w_i} = \frac{M(x_i^* \leftarrow x_{i+1}^*) \bar{P}(x_{i+1}^*)}{M(x_{i+1} \leftarrow x_i) \bar{P}(x_i)}, \quad (12)$$

where the conjugated point x_i^* is obtained from x_i inverting the momenta, i.e., if $x = (p, q)$, $x^* = (-p, q)$. If the dynamics exactly satisfies the detailed balance one must have $w_{i+1}/w_i = 1$, which implies that w must be constant. However, if $\bar{P}(x)$ is sampled in an approximated way, the degree to which w is constant can be used to assess the accuracy of the sampling.

Rather than in terms of weights, it is convenient to express this principle in terms of an effective energy

$$\tilde{H}_i = -\frac{1}{\beta} \ln w_i. \quad (13)$$

The evolution of \tilde{H} is given by

$$\begin{aligned} \tilde{H}_{i+1} - \tilde{H}_i &= -\frac{1}{\beta} \ln \left(\frac{M(x_i^* \leftarrow x_{i+1}^*) \bar{P}(x_{i+1}^*)}{M(x_{i+1} \leftarrow x_i) \bar{P}(x_i)} \right) \\ &= -\frac{1}{\beta} \ln \left(\frac{M(x_i^* \leftarrow x_{i+1}^*)}{M(x_{i+1} \leftarrow x_i)} \right) + H(x_{i+1}) - H(x_i), \end{aligned} \quad (14)$$

where the last line follows in the case of a canonical distribution $\bar{P}(x) \propto e^{-\beta H(x)}$.

Let us now make use of this result in the context of our dynamics. This is most conveniently achieved if we solve the equations of motion alternating two steps. One is a velocity Verlet step or any other area-preserving and time-reversible integration algorithm. In a step with such property, $M(x_i \leftarrow x_{i+1}^*) = M(x_{i+1} \leftarrow x_i)$ and the change in \tilde{H} is equal to the change in H . The other is a velocity-rescaling step in which the scaling factor is determined via Eq. (7). If we use the exact solution of Eq. (7) derived in the Appendix, this step satisfies the detailed balance and therefore does not change \tilde{H} . An idealized but realistic example of time evolution of H and \tilde{H} is shown in Fig. 1.

If we use this analysis and go to the limit of an infinitesimal time step, we find

$$\tilde{H}(t) = H(t) - \int_0^t (\bar{K} - K(t')) \frac{dt'}{\tau} - 2 \int_0^t \sqrt{\frac{K(t') \bar{K}}{N_f}} \frac{dW(t')}{\sqrt{\tau}}, \quad (15)$$

where the last two terms come from the integration of Eq. (7) along the trajectory. Note that a similar integration along the path is present in $H_{\text{Nosé}}$. However, in our scheme a stochastic integration is also necessary. In the continuum limit the changes in energy induced by the rescaling compensate exactly the fluctuations in H . For a finite time step this compensation is only approximate and the conservation of \tilde{H} provides a measure on the accuracy of the integration. This accuracy has to be interpreted in the sense of the ability of generating configurations representative of the ensemble. The physical meaning of Eq. (15) is that the fluxes of energy between the system and the thermostat are exactly balanced.

A further use of \tilde{H} is possible whenever high accuracy results are needed and even the small error derived from the use of a finite time-step integration needs to be eliminated. In practice, one can correct this error by reweighting¹⁶ the points with $w_i \propto e^{-\beta \tilde{H}_i}$. Alternatively, segments of trajectories can be used in a hybrid Monte Carlo scheme¹⁷ to generate new configurations which are accepted or rejected with probability $\min(1, e^{-\beta(\Delta \tilde{H})})$.

From the discussion above one understands that in many ways \tilde{H} has a role similar to E in the microcanonical ensemble. It is, however, deeply different: while in the microcanonical ensemble E defines the ensemble and has a physical meaning, in the canonical ensemble the value of \tilde{H} simply depends on the chosen initial condition. Thus, the value of \tilde{H} can be only compared for points belonging to the same trajectory.

III. APPLICATIONS

In this section we present a number of test applications of our thermostating procedure. Moreover, we compare its properties with those of commonly adopted thermostats, such as the Nosé-Hoover and the Berendsen thermostat. To test the efficiency of our thermostat, we compute the energy fluctuations and the dynamic properties of two model systems, namely, a Lennard-Jones system and water, in their crystalline and liquid phases. All the simulations have been performed using a modified version of the DL POLY code.^{18,19}

We adopt the parameterization of the Lennard-Jones potential for argon, and we simulate a cubic box containing 256 atoms. Calculations have been performed on the crystalline solid fcc phase at a temperature of 20 K and on the liquid phase at 120 K. The cell side is 21.6 Å for the solid and 22.5 Å for the liquid. Water is modeled through the commonly used TIP4P potential.²⁰ water molecules are treated as rigid bodies and interact via the dispersion forces and the electrostatic potential generated by point charges. The long-range electrostatic interactions are treated by the particle mesh Ewald method.²¹ The energy fluctuations and the dynamic properties, such as the frequency spectrum and the diffusion coefficient, have been computed on models of liq-

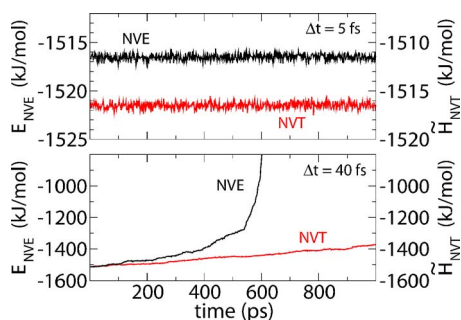


FIG. 2. (Color online) Total energy E (left axis) and effective energy \tilde{H} (right axis), respectively, for an NVE simulation and for an NVT simulation using our thermostat, with $\tau=0.1$ ps, for Lennard-Jones at 120 K. In the upper panel, the calculation is performed with a time step $\Delta t=5$ fs, and E (or \tilde{H}) does not drift. In the lower panel, the calculation is performed with a time step $\Delta t=40$ fs and E (or \tilde{H}) drifts.

uid water and hexagonal ice I_h , in cells containing 360 water molecules with periodic boundary conditions. The model of ice I_h , with a fixed density of 0.96 g/cm^3 , has been equilibrated at 120 K, while the liquid has a density of 0.99 g/cm^3 and is kept at 300 K.

A. Controlling the integration time step

As discussed in Sec. II C, the effective energy \tilde{H} can be used to verify the sampling accuracy and plays a role similar to the total energy in the microcanonical ensemble. In Fig. 2 we show the time evolution of \tilde{H} for the Lennard-Jones system at 120 K with two different integration time steps, namely, $\Delta t=5$ fs and $\Delta t=40$ fs. In both cases, we use $\tau=0.1$ ps for the thermostat time scale. With $\Delta t=5$ fs the integration is accurate and the effective energy \tilde{H} is properly conserved, in the sense that it does not exhibit a drift. Moreover, its fluctuations are rather small, approximately 0.3 kJ/mol: for a comparison, the root-mean-square fluctuations in H are on the order of 16 kJ/mol. When the time step is increased to $\Delta t=40$ fs, the integration is not accurate and there is a systematic drift in the effective energy. For a comparison we show also the time evolution of E in a conventional NVE calculation. The fluctuations and drifts for E in the NVE calculation are similar to the fluctuations and drifts for \tilde{H} in the NVT calculation. We notice that, while in the NVE calculation the system explodes at some point, the NVT calculation is always stable, thanks to the thermostat. However, in spite of the stability, the drift in \tilde{H} indicates that the sampling is inaccurate under these conditions.

B. Energy fluctuations

While the average properties are equivalent in all the ensembles, the fluctuations are different. Thus we use the square fluctuations of the configurational and kinetic energies, which are related to the specific heat of the system,¹ to check whether our algorithm samples the canonical ensemble. Therefore we perform 1 ns long molecular dynamics runs using our thermostat with different choices of the parameter τ , spanning three orders of magnitude. An integration time step $\Delta t=5$ fs is adopted, which yields a satisfactory

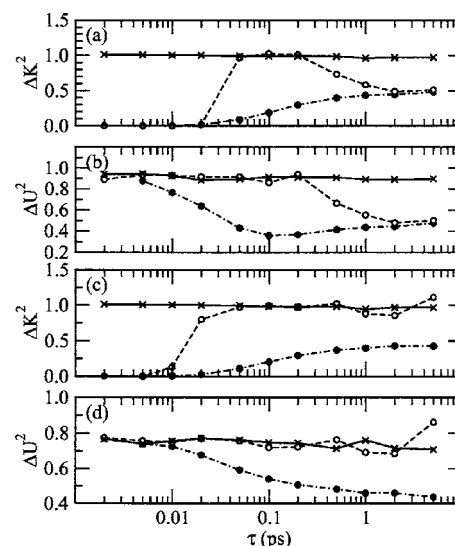


FIG. 3. Square fluctuations of the kinetic energy ΔK^2 and of the potential energy ΔU^2 , in units of $N_B k_B^2 T^2/2$, for a Lennard-Jones solid at 20 K [panels (a) and (b)] and liquid at 120 K [panels (c) and (d)], using the Berendsen (●, dashed-dotted), the Nosé-Hoover (○, dashed) and our (×, solid) thermostat, plotted as function of the characteristic time of the thermostat τ . In these units the analytical value for the fluctuations of the kinetic energy is 1.

conservation of the effective energy, as verified in the previous section. For comparison, we also calculate the fluctuations using the Nosé-Hoover thermostat, which is supposed to sample the proper ensemble. The results for the Lennard-Jones system, both solid and liquid, are presented in Fig. 3. The fluctuations are plotted in units of the ideal-gas kinetic-energy fluctuation. For the liquid [panels (c) and (d)], the Nosé-Hoover and our thermostat give consistent results for a wide range of values of τ for both the kinetic and configurational energy fluctuations. The Nosé-Hoover begins to fail only in the regime of small τ , due to the way the extra variable of the thermostat is integrated. For the solid [panels (a) and (b)], the ergodicity problems of the Nosé-Hoover thermostat appear for $\tau > 0.2$ ps, in terms of poor sampling. We notice that increasing τ , the fluctuations tend to their value in the microcanonical ensemble. On the other hand, our procedure is correct over the whole τ range, both for the solid and for the liquid. In Fig. 3 we also plot the fluctuations calculated using the Berendsen thermostat. It is clear that both for the liquid and for the solid the results are strongly dependent on the choice of the τ parameter. In the limit $\tau \rightarrow 0$ the Berendsen thermostat tends to the isokinetic ensemble, which is consistent with the canonical one for properties depending only on configurations;⁹ thus, the fluctuations in the configurational energy tend to the canonical limit, while the fluctuations in the kinetic energy tend to zero. In Fig. 4 we present a similar analysis done on water [panels (c) and (d)] and ice [panels (a) and (b)]. For this system the equations of motion have been integrated with a time step $\Delta t=1$ fs. In this case we only performed the calculation with the Nosé-Hoover thermostat and with ours. The Nosé-Hoover thermostat is not efficient for ice in the case of τ larger than 0.2 ps and also for water in the case of τ larger than 2 ps. On the other hand, the performance of our thermostat is again fairly independent from the choice of τ .

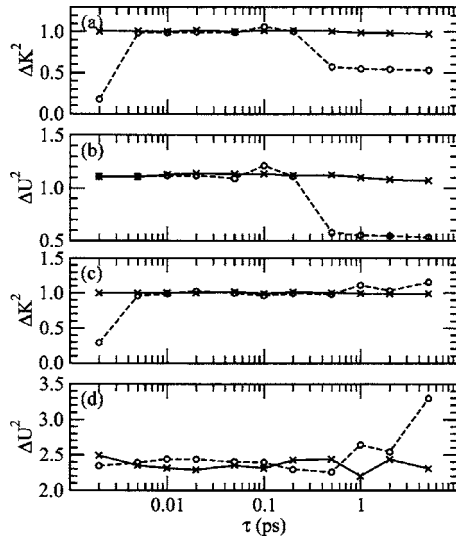


FIG. 4. Square fluctuations of the kinetic energy ΔK^2 and of the potential energy ΔU^2 , in units of $N_f k_B^2 T^2 / 2$, for ice at 120 K [panels (a) and (b)] and water at 300 K [panels (c) and (d)], using the Nosé-Hoover (\circ , dashed) and our (\times , solid) thermostat, plotted as function of the characteristic time of the thermostat τ . In these units the analytical value for the fluctuations of the kinetic energy is 1.

C. Dynamic properties

In order to check to what extent our thermostat affects the dynamic properties of the systems, we have computed the vibrational spectrum of the hydrogen atoms in ice I_h from the Fourier transform of the velocity-velocity autocorrelation function. The spectra have been computed, sampling 100 ps long trajectories in the NVT ensemble every 2 fs, at a temperature of 120 K, with two different values of the relaxation time τ of the thermostat (see Fig. 5). They are compared to the spectrum of frequencies obtained in a run in the microcanonical ensemble. In all these runs the integration time step Δt has been reduced to 0.5 fs. Two main regions can be distinguished in the vibrational spectrum of ice: a low frequency band corresponding to the translational modes (on the left in Fig. 5) and a band at higher frequency related to the librational modes. Due to the use of a rigid model the high frequency intramolecular modes are irrelevant. All the features of the vibrational spectrum of ice I_h are preserved

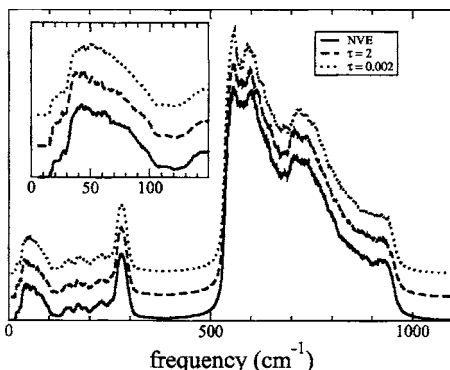


FIG. 5. Vibrational density of states for the hydrogen atom in ice I_h at 120 K. The spectra obtained with different values of the relaxation time τ of our thermostat (dashed and dotted lines) are compared to a simulation in the NVE ensemble (solid line).

TABLE I. The diffusion coefficient D of water at 300 K, as a function of the relaxation time τ of the thermostat. For a comparison, also the value obtained from an NVE trajectory is shown.

τ (ps)	D (10^{-5} cm ² /s)
0.002	3.63 ± 0.01
0.02	3.44 ± 0.06
0.2	3.51 ± 0.05
2.0	3.53 ± 0.01
NVE	3.47 ± 0.03

when our thermostat is used. When compared with the spectrum obtained from the NVE simulation, no shift of the frequency of the main peaks is observed for $\tau=2$ ps and the changes in their intensities are within numerical errors. It is worth noting that, although the thermostat acts directly on the particle velocities, it does not induce the appearance of fictitious peaks in the spectrum. The simulation done with $\tau=0.002$ ps shows that with a very short τ the shape of the first translational broad peak is slightly affected (see the inset in Fig. 5).

The performances of our thermostat have been tested also with respect to the dynamic properties of liquids, computing the self-diffusion coefficient D of TIP4P water. D is computed from the mean square displacement, through Einstein's relation, on 100 ps long simulations equilibrated at a temperature of 300 K. The results for different values of τ are reported in Table I and compared to the value of D extracted from an NVE simulation. The results obtained by applying our thermostat are compatible with the values of D reported in literature for the same model of water²² and are consistent with the one extracted from the microcanonical run. A marginal variation with respect to the reference value occurs for very small $\tau=0.002$ ps.

IV. CONCLUSION

We devised a new thermostat aimed at performing molecular dynamics simulations in the canonical ensemble. This scheme is derived from a modification of the standard velocity rescaling with a properly chosen random factor and generalized to a smoother formulation which resembles the Berendsen thermostat. Under the assumption of ergodicity, we proved analytically that our thermostat samples the canonical ensemble. Through a proper combination with a barostat, it can be used to sample the constant-pressure-constant-temperature ensemble. We check the ergodicity assumption on realistic systems and we compare the ergodicity of our procedure with that of the Nosé-Hoover thermostat, finding our method to be more ergodic. We also use the concept of sampling accuracy rather than trajectory accuracy to assess the quality of the numerical integration of our scheme. To this aim, we introduce a new quantity, which we dub effective energy, which measures the ensemble violation. This formalism allows a robust check on the finite time-step errors and can be easily extended to other kinds of stochastic molecular dynamics, such as the Langevin dynamics.

ACKNOWLEDGMENTS

The authors would like to thank Davide Branduardi for useful discussions. Also Gabriele Petraglio is acknowledged for carefully reading the paper.

APPENDIX: EXACT PROPAGATOR FOR THE KINETIC ENERGY

For the thermostat designed here it is essential that the exact solution of Eq. (7) is used. In the search for an analytical solution, we are inspired by the fact that if each individual momentum is evolved using a Langevin equation, then the evolution of K is described by the same Eq. (7). Thus we first define an auxiliary set of N_f stochastic processes $x_i(t)$ with the following equation of motion:

$$dx_i(t) = -\frac{x_i(t)}{2} \frac{dt}{\tau} + \frac{dW_i(t)}{\sqrt{\tau}}. \quad (\text{A1})$$

This is the equation for an overdamped harmonic oscillator which is known also as the Ornstein-Uhlenbeck processes for which an analytical solution exists:²³

$$x_i(t) = x_i(0)e^{-t/2\tau} + \sqrt{1 - e^{-t/\tau}} R_i, \quad (\text{A2})$$

where the R_i 's are independent random numbers from a Gaussian distribution with unitary variance. Then we define the variable y

$$y(t) = \frac{1}{N_f} \sum_{i=1}^{N_f} x_i^2(t). \quad (\text{A3})$$

The equation of motion for y is obtained applying the Itoh rules¹⁴ to Eq. (A1) and recalling that the increments dW_i are independent,

$$dy(t) = (1 - y(t)) \frac{dt}{\tau} + 2 \sqrt{\frac{y(t)}{N_f}} \frac{dW(t)}{\sqrt{\tau}}. \quad (\text{A4})$$

Since the equation of motion for x is invariant under rotation, we can assume without loss of generality that at $t=0$ the multidimensional vector $\{x_i\}$ is oriented along its first component,

$$\{x_i(0)\} = \{\sqrt{N_f}y(0), 0, \dots\}. \quad (\text{A5})$$

Combining Eqs. (A3) and (A2) we obtain for $y(t)$ at finite time,

$$y(t) = e^{-t/\tau} y(0) + (1 - e^{-t/\tau}) \sum_{i=1}^{N_f} \frac{R_i^2}{N_f} + 2e^{-t/2\tau} \sqrt{1 - e^{-t/\tau}} \sqrt{\frac{y(0)}{N_f}} R_1. \quad (\text{A6})$$

We now observe that with the substitution $y(t) = K_t/K$, Eq. (A4) is equivalent to Eq. (7). Thus, with simple algebra, we

find the desired expression for the rescaling factor,

$$\alpha^2 = e^{-\Delta t/\tau} + \frac{\bar{K}}{N_f K} (1 - e^{-\Delta t/\tau}) (R_1^2 + \sum_{i=2}^{N_f} R_i^2) + 2e^{-\Delta t/2\tau} \sqrt{\frac{\bar{K}}{N_f K}} (1 - e^{-\Delta t/\tau}) R_1. \quad (\text{A7})$$

We observe here that there is no need to draw all the R_i 's Gaussian numbers, because $\sum_{i=2}^{N_f} R_i^2$ can be drawn directly from the Gamma distribution $p_{(N_f-1)/2}(x) = x^{(N_f-1)/2-1} e^{-x} / \Gamma((N_f-1)/2)$ if N_f-1 is even or by adding a squared random Gaussian number to that extracted from $p_{(N_f-2)/2}(x) = x^{(N_f-2)/2-1} e^{-x} / \Gamma((N_f-2)/2)$ if N_f-1 is odd.²⁴ A routine that evaluates Eq. (A7) is available upon request.

- ¹M. P. Allen and D. J. Tildesley, *Computer Simulation of Liquids* (Oxford University Press, Oxford, 1987).
- ²D. Frenkel and B. Smit, *Understanding Molecular Simulation*, 2nd ed. (Academic, New York, 2002).
- ³H. C. Andersen, J. Chem. Phys. **72**, 2384 (1980).
- ⁴T. Schneider and E. Stoll, Phys. Rev. B **17**, 1302 (1978).
- ⁵D. M. Heyes, Chem. Phys. **82**, 285 (1983).
- ⁶S. Nosé, J. Chem. Phys. **81**, 511 (1984).
- ⁷W. G. Hoover, Phys. Rev. A **31**, 1695 (1985).
- ⁸G. J. Martyna, M. L. Klein, and M. Tuckerman, J. Chem. Phys. **97**, 2635 (1992).
- ⁹D. J. Evans and G. P. Morriss, Comput. Phys. Rep. **1**, 297 (1984).
- ¹⁰H. J. C. Berendsen, J. P. M. Postma, W. F. van Gunsteren, A. DiNola, and J. R. Haak, J. Chem. Phys. **81**, 3684 (1984).
- ¹¹Y. Sugita and Y. Okamoto, Chem. Phys. Lett. **314**, 141 (1999).
- ¹²V. I. Manousiouthakis and M. W. Deem, J. Chem. Phys. **110**, 2753 (1999).
- ¹³W. C. Swope, H. C. Andersen, P. H. Berens, and K. R. Wilson, J. Chem. Phys. **76**, 637 (1982).
- ¹⁴C. W. Gardiner, *Handbook of Stochastic Methods*, 3rd ed. (Springer, New York, 2003).
- ¹⁵T. Soddemann, B. Dünweg, and K. Kremer, Phys. Rev. E **68**, 046702 (2003).
- ¹⁶W. H. Wong and F. Liang, Proc. Natl. Acad. Sci. U.S.A. **94**, 14220 (1997).
- ¹⁷S. Duane, A. D. Kennedy, B. J. Pendleton, and D. Roweth, Phys. Lett. B **195**, 216 (1987).
- ¹⁸W. Smith, M. Leslie, and T. R. Forester, DL POLY code, Version 2.16, CCLRC Daresbury Laboratory, Daresbury, England.
- ¹⁹W. Smith and T. R. Forester, J. Mol. Graphics **14**, 136 (1996).
- ²⁰W. L. Jorgensen, J. Chandrasekhar, J. F. Madura, R. W. Impey, and M. L. Klein, J. Chem. Phys. **79**, 926 (1983).
- ²¹T. Darden, D. York, and L. Pedersen, J. Chem. Phys. **98**, 10089 (1993).
- ²²D. van der Spoel, P. J. van Maaren, and H. J. C. Berendsen, J. Chem. Phys. **108**, 10220 (1998).
- ²³H. Risken, *The Fokker-Planck Equation*, 2nd ed. (Springer, New York, 1989).
- ²⁴W. H. Press, S. A. Teukolsky, W. T. Vetterling, and B. P. Flannery, *Numerical Recipes in FORTRAN: The Art of Scientific Computing*, 2nd ed. (Cambridge University Press, Cambridge, 1992).